Available online at www.sciencedirect.com
SCIENCE DIRECT®
Pergamon
Cement and Concrete Research 33 (2003) 1257–1262
CEMENT AND CONCRETE RESEARCH

Characterization of mercury- and zinc-doped alkali-activated slag matrix Part II. Zinc

Guangren Qian[a,*], Darren Delai Sun[b], Joo Hwa Tay[b]

[a]School of Environment Engineering, Shanghai University, No. 149 Yanchang Road, Shanghai 200072, PR China
[b]Environmental and Engineering Research Center, School of Civil and Environment Engineering, Nanyang Technological University, Singapore, Singapore

Received 6 June 2002; accepted 31 January 2003

Abstract

The compressive strength, setting time, pore structure and hydration product of Zn-doped, alkali-activated slag (AAS) matrix have been investigated by examination of physical properties, micropore analysis, thermal analysis, FTIR, SEM and TCLP methods. The results show that the effects of Zn^{2+} on the AAS matrix depend on Zn^{2+} ion concentrations. At low Zn^{2+} ion concentrations, little negative influences on the compressive strength, setting time and distribution of pore structure were observed. Moreover, low concentrations of Zn^{2+} ion could be effectively immobilized in the AAS matrix. For 2% Zn-doped AAS matrix, the hydration of AAS paste was greatly retarded and leaching from this matrix was higher than TCLP zinc limit even at 28 days. Based on the analyses of hydration products, the chemical fixation mechanisms are considered responsible for the immobilization of Zn^{2+} ions in the AAS matrix.

Keywords: Zinc; Immobilization; Alkali-activated slag matrix; Hydration products and physical properties

1. Introduction

In a previous companion paper, Part I [1], both physical encapsulation and chemical binding mechanisms were considered responsible for the immobilization of mercury in the alkali-activated slag (AAS) matrix.

The effects of Zn on ordinary cement-based solidification have been extensively studied. As noted, soluble zinc salts added to ordinary Portland cement (OPC) cause the retardation of hydration and the decrease of strength, especially at concentrations above 0.3 wt.% [2–4]. The main mechanisms of retardation for Zn^{2+} in the OPC matrix may be summarized as follows: (1) sorption onto high surface area of C-S-H, (2) hydroxide precipitation due to high pH and (3) incorporation into calcium silicate hydrate C-S-H.

Cock et al. [5] showed that zinc from solution is adsorbed onto the surface of cement particles and inhibits the hydration of cement and silicate polymerisation [6]. In a high-pH, aqueous environment, the soluble zinc salts easily exist as zinc hydroxy anions $Zn(OH)_3^-$ and $Zn(OH)_4^{2-}$ [7]. These zinc hydroxy anions are transformed into calcium zincate phase $CaZn_2(OH)_6{\cdot}2H_2O$, which completely covers the cement grains, and thus passivates them from further hydration [8,9]. Mollah et al. [10] suggested that the formation of calcium zincate controls the solubility of zinc. Additionally, the mechanism of fixation at low concentrations differs from that at high concentrations. In the case of low concentrations, zinc could be nearly incorporated into the C-S-H without other products [11]. The site of incorporation may be either replacement of Ca^{2+} [12] or linked directly at the end of the silicate chains through Zn-O-Si bonds [11,13].

As reported in Part I, AAS matrix is quite different from the OPC matrix, but the full picture for the Zn-doped AAS matrix is hardly known. The present work will deal with the effects of Zn salt on the hydration, mechanical properties and microstructures of AAS matrix.

2. Experiments

2.1. Materials and immobilization matrixes

The blast furnace slag used for AAS matrix was from Malaysia Steel and Iron Corporation. The chemical com-

* Corresponding author. Fax: +86-21-56333052.
E-mail address: grqiang@mail.shu.edu.cn (G. Qian).

0008-8846/03/$ – see front matter © 2003 Elsevier Science Ltd. All rights reserved.
doi:10.1016/S0008-8846(03)00046-2

position of this slag is as follows: 40.31% CaO, 34.47% SiO_2, 9.47% Al_2O_3, 0.53% Fe_2O_3 and 7.81% MgO. This slag had a specific surface of 480 m^2/kg. All the pastes of solidification matrix were prepared with a sodium silicate solution/slag ratio of 0.3. The SiO_2/Na_2O of alkali solution was kept at 2.0 by addition of NaOH. Four dosages of Zn^{2+} ions, 0%, 0.1%, 0.5% and 2.0% by mass of the slag, were added with $Zn(NO_3)_2{\cdot}6H_2O$ salt into alkali solution and then corresponding cubes ($50 \times 50 \times 50$ mm) were made. All specimens were cured at room temperature and 100% relative humidity for 1, 3, 7, 14 and 28 days.

2.2. Examination of physical properties tests and leaching test

The setting times and compressive strengths of Zn-doped AAS matrixes cured at different ages were measured by ASTM C191-2001 and ASTM C109-2001. The leaching properties for these matrixes were evaluated by EPA-1311 method. The Zn^{2+} ion concentrations in the filtered solution were measured by inductively coupled plasma emission spectrometry (ICP-OES).

2.3. Characterization of hydration products

After the strength test, the specimens were crushed into coarse particles or powder and treated with an acetone–alcohol solution for stopping the hydration. TG, DSC, IR and SEM methods were used to identify the hydration products of harden matrixes. The pore size distributions of matrixes were determined by Micromeritics Autopore III.

3. Results and discussion

3.1. Physical properties

The setting times and compressive strength developments of Zn-doped AAS matrixes are illustrated in Figs. 1 and 2, respectively. Effects of Zn^{2+} on the physical properties of AAS matrixes were sensitive to its dosage. At 0.1% Zn^{2+} ion dosage, negative effects were hardly found. The setting time and compressive strength developments for 0.1% Zn-AAS matrix were nearly the same as that of pure AAS matrix. As for 0.5% Zn-AAS, the setting times were slightly prolonged by 10–20 min and the compressive strengths at 3 and 7 days were down by 10–20%. However, 2% Zn^{2+} addition had obvious negative influences on the physical properties of AAS matrix. The paste of this matrix had a much slower setting: 248 min for initial setting and 467 min for final setting. It suggests that the rapid setting of pure AAS matrix could be adjusted by suitable Zn salt addition. In addition, 2% Zn-AAS matrix presented a quite poor compressive strength, 2–3 MPa from 7 to 14 days and 9.5 MPa at 28 days, indicating that this matrix only preserved 13% of compressive strength compared to pure

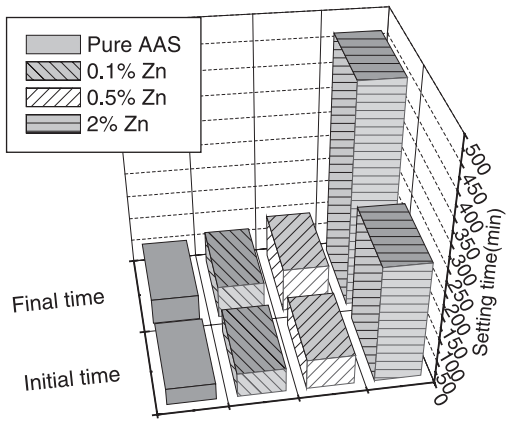

Fig. 1. Setting times of Zn-doped AAS matrixes.

AAS matrix at 28 days. In contrast, 2% Zn-OPC matrix could keep 75% of compressive strength compared to pure OPC matrix at 28 days. These results indicate that the strength development of AAS matrixes would be more strongly depressed by Zn^{2+} addition than that of OPC matrix.

3.2. Pore size distribution

Cumulative pore size distributions of Zn-AAS matrixes are shown in Fig. 3. The 0.5% Zn-doped AAS matrix, which was cured for 28 days, had an equiform pore size distribution as pure AAS matrix and they all had about 11% of total pore volume. As for 2% Zn-AAS matrix, the total pore volume was not evidently reduced from 7 to 28 days and lay at 20–23%, similar to that of OPC matrixes. Moreover, the shape of pore size distribution for 2% Zn-AAS matrix was quite different from that of 0.5% Zn-AAS matrix.

The pore size distributions of matrixes could be quantitatively condensed into micropore (>500 nm) and mesopore (<500 nm) according to the procedure described in Part I. Fig. 4 illustrates the calculated results. The 0.5% Zn-AAS matrix had 74% of mesopore, similar to pure AAS matrix. For 2% Zn-AAS matrix, the volume of mesopore was 15% at 7 days and increased to 31% at 28 days. It means that the micropore predominates over the pore structure of 2% Zn-AAS matrix through its hardening process.

3.3. TCLP leaching tests

The leached Zn^{2+} ion concentrations in TCLP extracts for Zn-doped AAS matrixes are listed in Table 1. As the concentrations of Zn^{2+} ion in the AAS matrix were below 0.5%, the leaching values of matrix cured for less than 3 days were over 5.0 mg/l of the threshold limit, 6–81 mg/l; then rapidly decreased to 0.24–1.18 mg/l after curing for 7 days, far below the TCLP threshold limit. In the case of 2% Zn^{2+} addition, the leaching of matrix cured for 3 days was as high as 1954 mg/l and decreased to 673 and 44 mg/l at 7 and 14

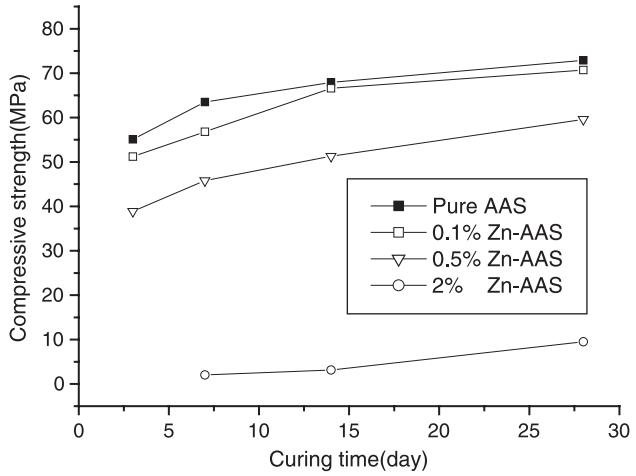

Fig. 2. Compressive strengths of Zn-doped AAS matrixes as a function of curing time.

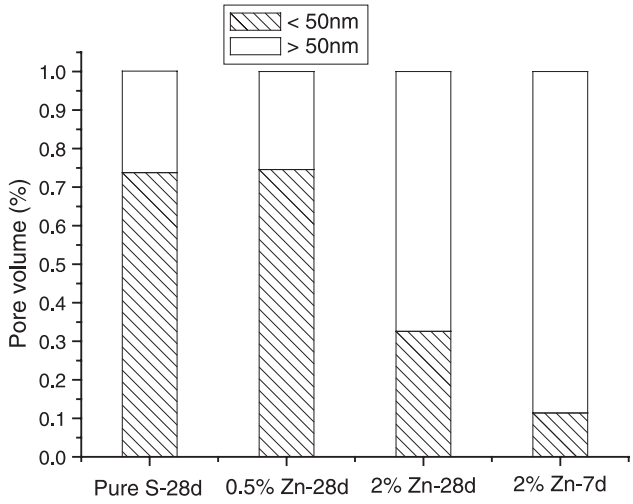

Fig. 4. Mesopore and micropore distributions of Zn-doped AAS matrixes.

days, respectively. Even at 28 days, 2% Zn-AAS matrix had 9.06 mg/l leaching, still much higher than 5.0 mg/l.

Although the leaching from 2% Zn-AAS matrix at 28 days cannot meet the TCLP threshold limit, in fact, over 99.99% Zn^{2+} ions had been fixed in the AAS matrix because the addition of 2% Zn^{2+} means that about 60,000 ppm of Zn^{2+} ions were added into the AAS matrix. As judged by its compressive strength and pore distributions, therefore, the physical encapsulation mechanism was impossible to immobilize such a high concentration of Zn^{2+} ions in the AAS matrix.

3.4. Hydration products

The hydration products of Zn-doped AAS matrixes were identified by TG-DTG, DSC, FTIR and SEM.

3.4.1. TG-DTG and DSC

Fig. 5 shows TG-DTG curves of Zn-doped matrixes cured for 28 days. The characteristics of TG-DTG curves

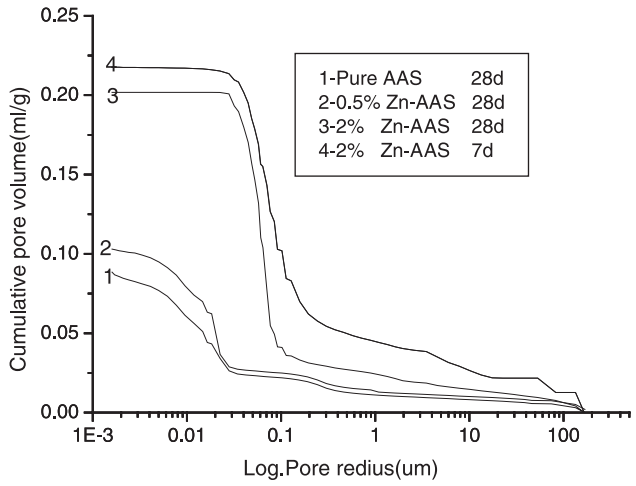

Fig. 3. Cumulative pore size distributions of Zn-doped AAS matrixes.

for three matrixes, 0%, 0.1% and 0.5% Zn-AAS, have no obvious differences. The 2% Zn-AAS matrix gave quite smaller weight loss at 28 days than the above three matrixes. As the degree of hydration for Zn-AAS matrix could be approximately and quantitatively estimated by their weight losses, it was found that the hydration degree of 2% Zn-AAS matrix was only 47% of pure AAS matrix at 28 days, which further proves that 2% Zn^{2+} greatly retarded the hydration of AAS matrix.

The weight losses for 2% Zn-AAS matrix at different ages are recorded in Fig. 6. At 3 and 7 days, this matrix had a sudden weight loss between 520 and 610 °C with DTG peak centered at 565 °C, apart from a sharp weight loss of free water at around 100 °C. According to Maliavski et al. [14], this weight loss at around 565 °C should be attributed to the decomposition of amorphous zinc silicate gel. At 14 days, the weight loss from zinc silicate gel was still strong and another new DTG peak occurred at around 165 °C. This peak may be due to the decomposition of calcium zincate, indicating calcium zincate began to form at that time. At 28 days, the weight loss from zinc silicate gel became less strong but that from calcium zincate was somewhat stronger than at 14 days. Compared to 2% Zn-AAS matrix, the matrixes with 0.1% and 0.5% Zn^{2+} additions had no trace of calcium zincate phase at 28 days as no weight loss around 165 °C was detected in Fig. 5.

Fig. 7 shows DSC curves of Zn-AAS matrixes cured for 7 and 28 days. When cured for 28 days, both 0.5% and 2%

Table 1
Leaching of Zn^{2+} ions from Zn-doped AAS matrix by TCLP tests

Curing time (days)	Leaching of Zn^{2+} (mg/l)		
	0.1% Zn^{2+}	0.5% Zn^{2+}	2.0% Zn^{2+}
1	24.21	381.49	1870.32
3	6.51	13.42	1954.15
7	0.24	1.18	673.72
14	0.026	0.042	44.78
28	0.011	0.029	9.06

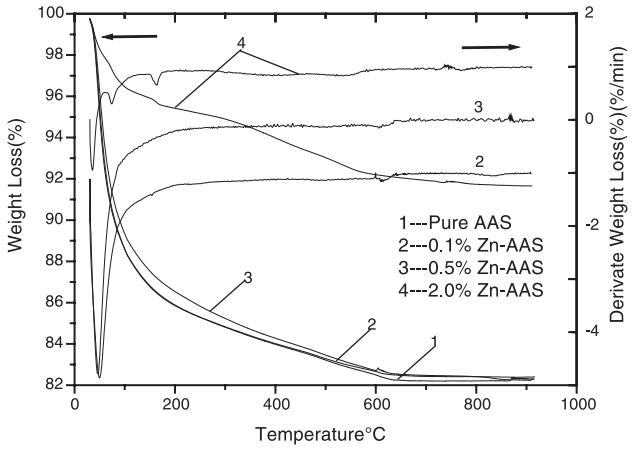

Fig. 5. TG-DTG curves of Zn-doped AAS matrixes cured for 28 days.

Zn-AAS matrixes showed an exothermic peak at 815 and 775 °C, respectively. This exothermic peak corresponds to the decomposition of calcium silicate hydrate C-S-H into wollastonite phase. The decomposition temperature of C-S-H from 2% Zn-AAS was apparently lower than that from 0.5% Zn-AAS matrix. Whether it means that more Zn^{2+} ions were incorporated into C-S-H is unknown. As 2% Zn-AAS matrix was cured for 7 days, however, this exothermic peak from C-S-H did not appear, indicating that the formation of C-S-H was greatly inhibited by more Zn^{2+} salt addition at early age.

It is also observed in Fig. 7 that 2% Zn-AAS matrixes cured for 7 and 28 days showed a poor endothermic peak of DSC around 558–568 °C, which could further support the presence of zinc silicate gel. Moreover, 2% Zn-AAS matrix at 28 days had another endothermic peak at 180 °C, which should be identical with the weight loss peak around 165° C in Fig. 5, confirming the presence of the calcium zincate phase. As a comparison, none of the two endothermic peaks from zinc silicate gel and calcium zincate were observed for 0.5% Zn-AAS matrix.

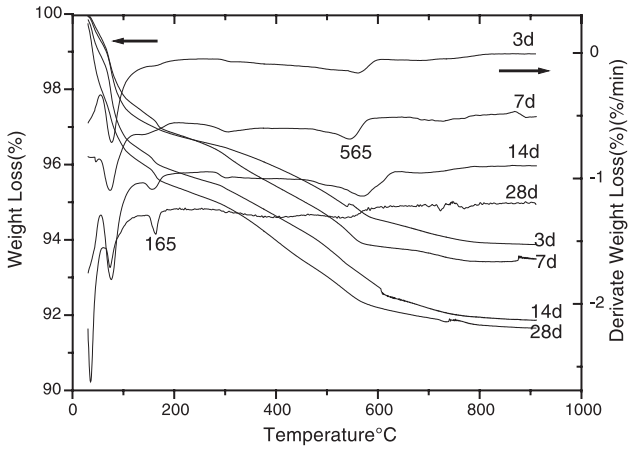

Fig. 6. TG-DTG curves of 2% Zn-doped AAS matrixes cured for different ages.

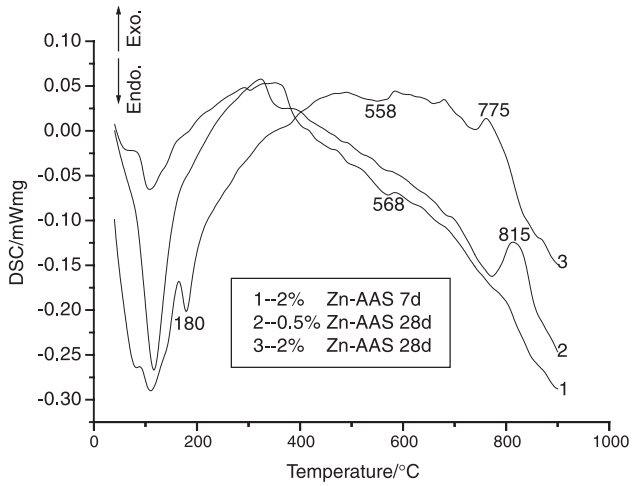

Fig. 7. DSC curves of Zn-doped AAS matrixes.

3.4.2. FTIR

FTIR spectra of Zn-doped AAS matrixes cured for 28 days are shown in Fig. 8. Mollah et al. [10] established that OH stretching bands at the highest frequencies, 3652 and 3637 cm^{-1}, could be used as a good proof of calcium zincate presence. Although the presence of calcium zincate in 2% Zn-AAS matrix has been detected by TG and DSC, no splitting of the OH stretching band at 3400–3600 cm^{-1} occurred and only a broad trough band around 3500 cm^{-1} was recorded. In fact, this broad band may be overlapped with several OH stretching bands from C-S-H, zinc silicate gel and calcium zincate. On the other hand, the ν_3 absorption band for 0.1% Zn-AAS matrix was at 971 cm^{-1} and this band was shifted to 975 cm^{-1} for 0.5% Zn-AAS matrix. Apparently, this shift toward high wave numbers coincided well with the increases of Zn^{2+} addition in the AAS matrixes and was similar to that of Hg-doped AAS matrixes. As discussed in Part I, the ν_3 absorption band of Si-O-Si is sensitive to the vibration of linkages between Si-O-Si tetrahedra and surrounding secondary building blocks of structure. The XAF experiments of Moulin et al. [13] showed that Zn tetrahedra are incorporated within the C-S-H

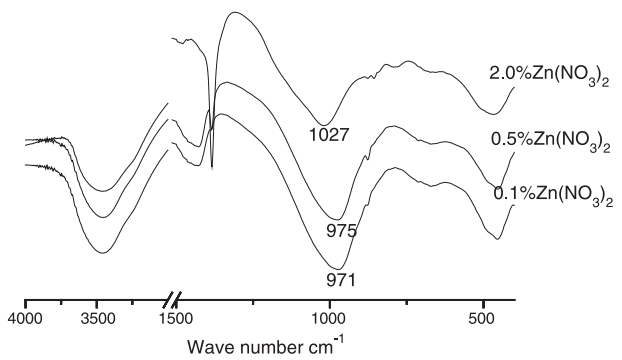

Fig. 8. IR spectra of Zn-doped AAS matrixes cured for 28 days.

matrix and linked directly at the end of the silicate chains through Zn-O-Si bonds, whereas Komarneni et al. [12] suggested that heavy metal cations could substitute for Ca^{2+} during the incorporation into the C-S-H. Whatever the exact positions of Zn immobilization in the C-S-H were, it may be sure that the surrounding linkages of Si-O-Si tetrahedra in the C-S-H were modified by the incorporation of Zn^{2+} ion so that the more the incorporation of Zn^{2+} ion, the more the shift of the ν_3 band.

The ν_3 absorption band for 2% Zn-doped AAS matrix was further shifted to 1027 cm^{-1}. Apart from more Zn^{2+} incorporated in C-S-H, this higher wave number may be overlapped with the ν_3 absorption band of unhydrated slag in the matrix.

3.4.3. SEM

The morphology of hydration products for Zn-doped AAS matrixes cured for 28 days are shown in Fig. 9. The 0.5% Zn-AAS matrix produced many fine flake-like hydration products 1–2 μm long. By XRD, TG and FTIR, these products should be attributed to poorly crystallized C-S-H. However, the morphology of hydration products for 2% Zn-AAS matrix was not easily distinguished. An amorphous product layer covered the surface of all the particles and there still existed many visible voids among the particles.

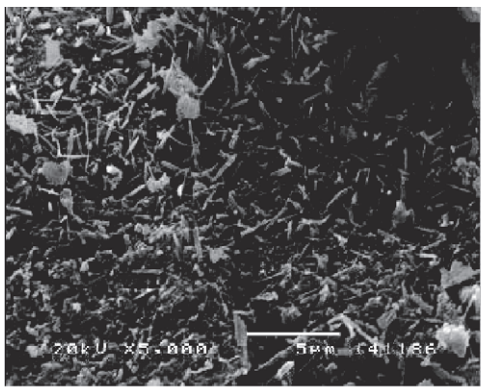

(a)

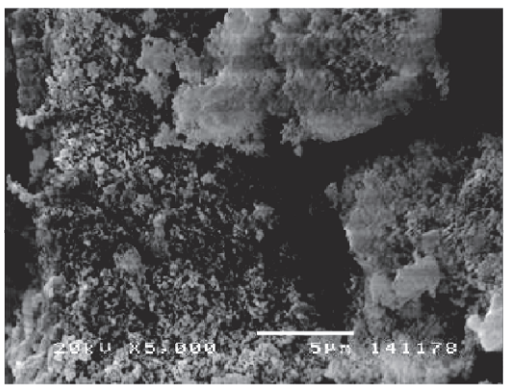

(b)

Fig. 9. Morphology of hydration products for Zn-doped AAS matrixes at 28 days. (a) 0.5% Zn-AAS matrix, (b) 2% Zn-AAS matrix.

These amorphous products are probably mixtures of zinc silicate gelatin and poorly crystallized C-S-H. It means that 2% Zn-AAS did not hydrate well even at 28 days and C-S-H products in this matrix had much poorer crystallization than other matrixes with low concentrations of Zn^{2+} ions.

4. Discussion

As described above, 2% Zn-doped AAS matrix had a quite low compressive strength and coarse pore structure. In this case, the physical encapsulation mechanism should not dominate over the effective immobilization of Zn^{2+} ions in the AAS matrix. Alternatively, the chemical stabilization mechanisms could be responsible for this.

Based on the results presented, the chemical stabilization mechanisms for immobilizing Zn^{2+} ion in the AAS matrix may involve (1) the formation of insoluble zinc silicate gel, (2) the incorporation of Zn^{2+} ion into the C-S-H lattice and (3) the formation of insoluble calcium zincate precipitate.

Firstly, as soon as zinc salt comes into contact with soluble sodium silicate solution, they immediately react with each other to form insoluble zinc silicate gelatin. At this moment, most of soluble Zn^{2+} ions are preferentially bound into this insoluble gelatin. Furthermore, this gelatinous zinc silicate would cover the outer surface of slag particles to inhibit the reaction of slag with soluble sodium silicate so that the hydration of Zn-AAS matrix is retarded. The degree of retardation depends on how many slag particles are covered with insoluble gelatinous layer.

Secondly, the slag particles uncovered with gelatin are easily react with free soluble sodium silicate and NaOH to form the same product C-S-H as pure AAS matrix. The aqueous solution in the sodium silicate–NaOH–slag system keeps a higher pH (around 11) on which the glass structure of slag would be disjointed so that Ca^{2+}, SiO_4^{4-} and AlO_4^{3-} ions are to be continuously released into aqueous solution. Consequently, formed zincate silicate gel may be attacked by Ca^{2+} and OH^- ions to form insoluble calcium zincate. Results showed that calcium zincate in 2% Zn-AAS matrix was formed after curing for 14 days. However, the exact course of formation of calcium zincate phase is not clear.

Thirdly, the formation of C-S-H during the hydration process would incorporate a part of Zn^{2+} ions into its lattice structure. The amount of Zn^{2+} ions bound into C-S-H is proportional to the amount of C-S-H formed in the matrix. At low Zn^{2+} ion concentrations, the formation of C-S-H was less hindered. Consequently, Zn^{2+} ions would be preferentially incorporated into the C-S-H and bound into insoluble zinc silicate phase. The results have proved that no calcium zincate was found for the AAS matrixes with less than 0.5% Zn^{2+} additions. For the OPC matrix, Rose et al. [11] gave a similar result that Zn^{2+} ion was only incorporated in the C-S-H framework without any precipitation products at low Zn^{2+} concentrations. For 2% Zn-doped

AAS matrix, however, Zn^{2+} ions may be predominantly combined with insoluble zinc silicate and calcium zincate due to the largely hindered formation of C-S-H.

5. Conclusions

(1) The effects of Zn^{2+} on the AAS matrix depend on Zn^{2+} ion concentrations. At low Zn^{2+} ion concentrations, little negative influences on the compressive strength, setting time and distribution of pore structure were observed. Moreover, low concentrations of Zn^{2+} could be effectively immobilized in the AAS matrix with the leaching satisfied for the TCLP zinc limit.
(2) For 2% Zn-doped AAS matrix, the hydration of AAS paste was still greatly retarded even at 28 days. Meanwhile, the leaching from this matrix was higher than the TCLP zinc limit.
(3) Chemical fixation mechanisms are responsible for the immobilization of Zn^{2+} ions in the AAS matrix. They include the formation of insoluble zinc silicate gel, the formation of insoluble calcium zincate precipitate and the incorporation of Zn^{2+} ions into the C-S-H lattice, depending on Zn^{2+} ion concentrations in the AAS matrixes.

References

[1] G.R. Qian, D.D. Sun, J.W. Tay, Characterization of mercury and zinc-doped alkali activated slag matrix: Part I. Mercury, Cem. Concr. Res. 33 (2003) 1251–1256.
[2] C.S. Poon, R. Perry, Study of zinc, cadmium and mercury stabilization in OPC/PFA mixtures, in: G.J. McCarthy, F.P. Glasser, D.M. Roy, S. Diamond (Eds.), Fly Ash and Coal Conversion By-products Characterization, Utilization and Disposal III, Materials Research Society Symposium Proceedings, vol. 86, Materials Research Society, Pittsburgh, 1987, pp. 67–77.
[3] D. Stephan, H. Maleki, D. Knofel, B. Eber, R. Hardtl, Influence of Cr, Ni and Zn on the properties of pure clinker phases: Part I. C3S, Cem. Concr. Res. 29 (1999) 545–552.
[4] I.F. Olmo, E. Chacon, A. Irabien, Influence of lead, zinc, iron (III) and chromium(III) oxides on the setting time and strength development of Portland cement, Cem. Concr. Res. 31 (2001) 1213–1219.
[5] D.L. Cocke, M.Y.A. Mollah, J.R. Parga, T.R. Hess, J.D. Ortego, An XPS and SEM/EDS characterization of leaching effects on Pb and Zn doped Portland cement, J. Hazard. Mater. 30 (1992) 83–95.
[6] J.D. Ortego, Y. Barroeta, F.K. Cartledge, H. Akhter, Leaching effects on silicate polymerisation, an FTIP and ^{29}Si NMR study of lead and zinc in Portland cement, Environ. Sci. Technol. 25 (1991) 1171–1174.
[7] M. Pourbaix, Atlas of Electrochemical Equilibria in Aqueous Solutions, National Association of Corrosion Engineers, Houston, TX, 1974.
[8] M.Y.A. Mollah, R.K. Vempati, T.C. Lin, D.L. Cocke, The interfacial chemistry of solidification/stabilization of metals in cement and pozzolantic material systems, Waste Manage. 15 (1995) 137–148.
[9] D.L. Cocke, M.Y.A. Mollah, The chemistry and leaching mechanisms of hazardous substances in cementitious solidification/stabilization systems, in: R.D. Spence (Ed.), Chemistry and Microstructure of Solidified Waste Forms, Lewis, Boca Raton, FL, 1993.
[10] M.Y.A. Mollah, J.R. Parga, D.L. Cocke, Infrared spectroscopic examination of cement-based solidification/stabilization systems—Portland types V and IP with zinc, J. Environ. Sci. Health, Part A, Environ. Sci. Eng. 27 (1992) 1503–1519.
[11] J. Rose, I. Moulin, A. Mason, P.N. Bertsch, M.R. Wiesner, J.Y. Bottero, F. Mosnier, C. Haehnel, X-ray spectroscopy study of immobilization process for heavy metals in calcium silicate hydrates: 2. Zinc, Langmuir 17 (2000) 3658–3665.
[12] S. Komarneni, E. Breval, D.M. Roy, R.R. Roy, Reactions of some calcium silicates with metal cations, Cem. Concr. Res. 18 (1988) 204–220.
[13] I. Moulin, W.E.E. Stone, J. Sanz, J.Y. Bottero, F. Mosnier, C. Haehnel, Lead and zinc retention during hydration of tri-calcium silicate: a study by sorption and ^{29}Si nuclear magnetic resource spectroscopy, Langmuir 15 (1999) 2829–2835.
[14] N.I. Maliavski, O.V. Dushkin, G. Scarinci, Low temperature synthesis of some orthosilicates, Ceram.-Silik. 45 (2001) 48–54.